Structural Modeling Of Pinna-Related Transfer Functions

Simone Spagnol spagnols@dei.unipd.it
Michele Geronazzo geronazz@dei.unipd.it
Federico Avanzini avanzini@dei.unipd.it
Università di Padova

ABSTRACT

This paper faces the general problem of modeling pinna-related transfer functions (PRTFs) for 3-D sound rendering. Following a structural *modus operandi*, we exploit an algorithm for the decomposition of PRTFs into ear resonances and frequency notches due to reflections over pinna cavities in order to deliver a method to extract the frequencies of the most important spectral notches. Ray-tracing analysis reveals a convincing correspondence between extracted frequencies and pinna cavities of a bunch of subjects. We then propose a model for PRTF synthesis which allows to control separately the evolution of resonances and spectral notches through the design of two distinct filter blocks. The resulting model is suitable for future integration into a structural head-related transfer function model, and for parametrization over anthropometrical measurements of a wide range of subjects.

1. INTRODUCTION

Back in 1907, Lord Rayleigh's Duplex Theory of Localization [1] gave birth to the vast and still little understood field of 3-D sound. As a matter of fact, the well-known diffraction formula which approximates the behaviour of a sound wave produced by an infinite point source around the listener's head provided a first glimpse of what we today call a head-related transfer function (HRTF). Nevertheless, compared to such centenary theory, most of the relevant issues in HRTF modeling are relatively recent.

There exists a number of ways to render HRTF-based spatial audio. Approximations based on low-order rational functions [2] and series expansions of HRTFs [3] were proposed, resulting in simple yet valuable tools for HRTF modeling. On the other hand the complexity of filter coefficients and weights, respectively, makes both techniques unsuitable for real-time applications. Conversely, structural modeling [4] seems nowadays to be an attractive alternative approach for all those scenarios where fast computation is needed: within this characterization, the contribution of the listener's head, ears and torso to the HRTF are isolated in several subcomponents, each accounting for some well-defined physical phenomenon. Thanks to linearity, the global HRTF can be later reconstructed from a proper combination of all these effects. The result of such a decomposition is a model which is both economical and well-suited to real-time implementations. Furthermore, the intuitive nature of physical parameters gives us the possibility of relating the model to anthropometrical measurements.

Our work focuses on the contribution of the pinna to the HRTF. Although perceptually dominated by head motion cues, pinna effects on incident sound waves are of great importance in sound spatialization. Several experiments have shown that, contrarily to azimuth effects which are dominated by diffraction around the listener's head and may be reduced to simple and intuitive binaural quantities, elevation cues are basically monaural and heavily depend on the listener's pinna shape, being the result of a superposition of scattering waves influenced by a number of resonant modes inside pinna cavities. Within this framework, it is crucial to find a suitable model for representing the pinna contribution to the HRTF, whose transfer function we commonly refer to as Pinna-Related Transfer Function (PRTF). In addition, linking the model parameters to straightforward anthropometric measurements on the user's pinnas is equally relevant and represents the ultimate challenge in this direction. Once such model is available, cascading it to a simple Head-and-Torso (HAT) model [5] would yield a complete structural HRTF representation.

In this paper we carry on the work presented in [6]. Exploiting an iterative approach which aims at separating resonance effects from pinna reflections in experimentally measured PRTFs, a method for extracting the frequencies of the most important notches is here sketched, followed by a discussion on the possible relation between notch frequencies and anthropometry. Finally, a structural model of the pinna is proposed.

2. PREVIOUS WORKS

Following Batteau's studies [7], high-frequency components which arrive at the listener's ear are typically reflected by the concha wall and rim, provided that their wavelength is small compared to the pinna dimensions. Due to interference between the direct and reflected waves, sharp notches can be observed in the incoming sound's spectrum at high frequencies with a periodicity of $1/\tau_i$, where τ_i is the time delay of the i-th reflection. Such observation led to a very simple double-path model of the pinna [8], whose main drawback lies in fixed reflection coefficients that overestimate the effective number of notches in the spectrum. Even so, the model's fit with experimental data was found to be reasonably good.

A similar approach was adopted by Barreto *et al.*, whose

model [9] consists in a reflection structure represented by four parallel paths, each modeled by a time delay τ_i and a magnitude factor ρ_i, cascaded to a low-order resonator block. As a matter of fact pinna cavities act as resonators, affecting the frequency content of both the direct and the reflected sound waves (see Shaw's work [10] for an extensive analysis of pinna resonant modes). The model parameters are fitted by decomposing each specific measured head-related impulse response (HRIR) into four scaled and delayed damped sinusoidal components using a procedure based on the second-order Steiglitz-McBride (STMCB) algorithm, and associating the delay and scaling factor of each component to the corresponding parameters of its associated path in the model. Multiple regression analysis was used in order to link the model parameters to eight measured anthropometric features [11]. Unfortunately, besides having no clear evidence of the physics behind the scattering phenomenon, the considered measures can only be obtained with the help of a 3-D laser scanner. Regardless of such particular concerns, this work surely certifies our final PRTF model's architecture, viz. a "resonance-plus-delay" structure.

The approach taken by Raykar *et al.* for reflection modeling [12] is different and operates both in the time and frequency domains. The authors used robust digital signal processing techniques based on the residual of a linear prediction model for the head-related impulse response (HRIR) to extract the frequencies of the spectral notches due to the pinna alone. Specifically, first the autocorrelation function of the HRIR's windowed LP residual is computed; then, frequencies of the spectral notches are found as the local minima of the group-delay function of the windowed autocorrelation. In addition, a ray-tracing argument was exploited to attest that the so found spectral notches are somehow related to the shape and anthropometry of the pinna. For each of the extracted notches the corresponding distance was plotted on the image of the pinna, and by varying elevation such mapping appeared consistent with reflections on the back of the concha and on the crus helias. Spectral peaks were extracted in parallel by means of a linear prediction analysis, yielding results which match quite well the pinna resonant modes reported by Shaw [10] and further justifying the "resonance-plus-delay" approach.

Hitherto, another significant contribution on low-cost modeling of PRTFs was provided by Satarzadeh *et al.* [13]. In this work PRTFs for elevation $\phi = 0^\circ$ are synthesized through a model composed of bandpass and comb filters, which respectively approximate the two major resonances (Shaw's resonant modes 1 and 4) and one main reflection. The two second-order bandpass filters and the comb filter are interconnected as in Figure 1, the latter taking the form $[1 + \rho \exp(-sT)]$, where T is the time delay of the considered reflection estimated from the spacing of notches in the PRTF spectrum and ρ a frequency-dependent reflection coefficient which strongly attenuates low-frequency notches, coming over Batteau's model aforementioned limitation. For what concerns the resonant part, a cylindrical approximation to the concha is used, where depth and width of the cylinder uniquely define the depth resonance, while

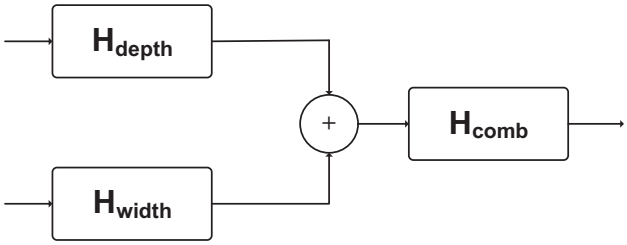

Figure 1. *The PRTF model proposed by Satarzadeh* et al. *[13].*

the width resonance is thought to be correlated to the time delay T depending on whether the concha or the rim is the significant reflector. Though the anthropometric significance of the two parameters is not robust, Satarzadeh claimed that if the pinna has an approximately cylindrical shaped concha and a structure with a dominant reflection area (concha or rim), his anthropometry-based filter provides a good fit to the experimental PRTF. In particular, it features sufficient adaptability to fit both PRTFs with rich and poor notch structures.

3. PRTF ANALYSIS

Taking the last two works described in the previous section as an inspiration and a "resonance-plus-delay" PRTF model as starting point, the main and final goal of our work is the construction of an essential multi-notch filter suitable for anthropometric parametrization. This obviously requires a PRTF analysis step. In order to analyze PRTFs, we consider measured HRIRs from the CIPIC database [14], a public domain database of high spatial resolution HRIR measurements at 1250 directions for 45 different subjects along with their anthropometry. We choose to investigate the behaviour of pinna features in subjects 010, 027, 134, and 165 in order to facilitate comparison with previous works on notch frequencies extraction (the same subjects' PRTFs were analyzed in [12]).

3.1 Pre-processing

For purpose of analysis we focus on HRIRs sampled on the median plane, with elevation varying from -45° to 90°. As a matter of fact, since sensitivity of PRTFs to azimuth is weak [13], we roughly expect PRTFs to be elevation dependent only. Such an assumption makes the PRTF model suitable for all azimuths.

Knowing that the magnitude response of an earless head with respect to a sound source in the median plane is ideally flat if the head is modeled as a rigid sphere, the only preprocessing step we apply to obtain a raw estimate of the PRTF is windowing the corresponding HRIR using a 1.0 ms Hann window [12]. In this way, spectral effects due to reflections caused by shoulders and torso are removed from the PRTF estimate.

In order to isolate the spectral notches in the so built PRTFs we exploit an ad-hoc designed algorithm that returns an estimate of the separated resonant and reflective components. The idea behind such algorithm is to itera-

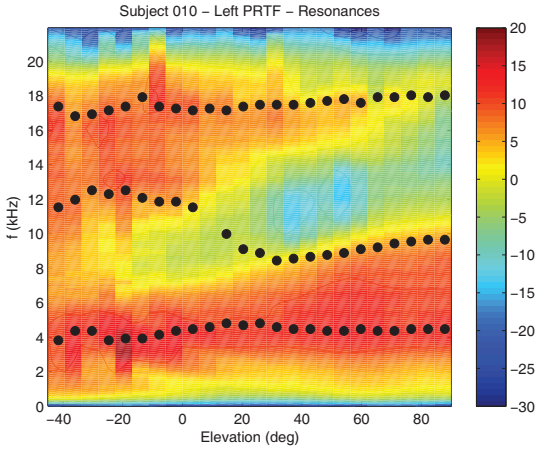

(a) Subject 010.

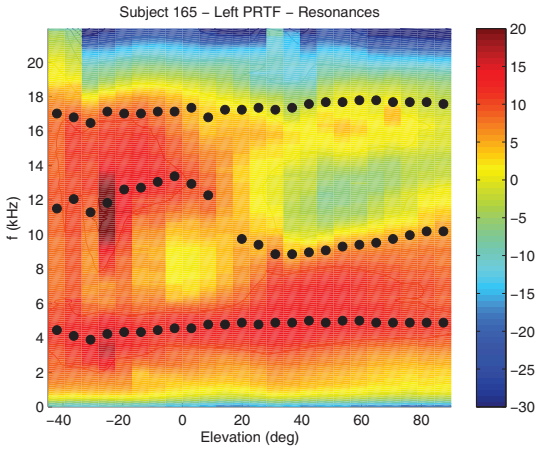

(b) Subject 165.

Figure 2. *Resonance plots for different elevations.*

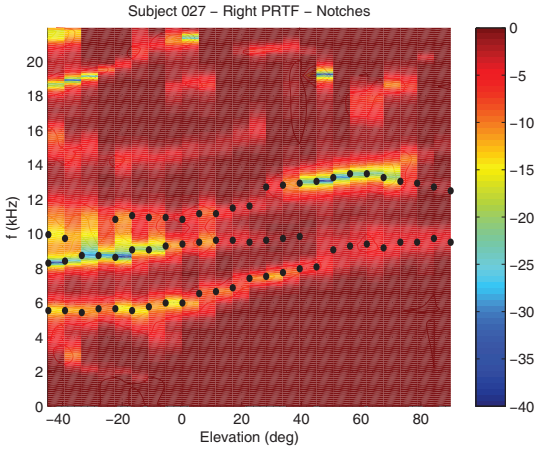

(a) Subject 027.

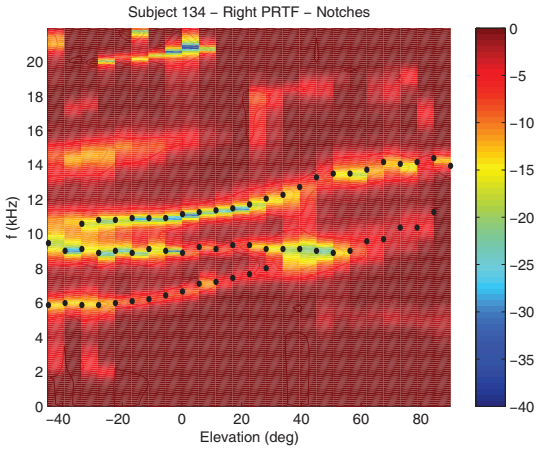

(b) Subject 134.

Figure 3. *Spectral notch plots for different elevations.*

tively compensate the PRTF magnitude spectrum with an approximate multi-notch filter until no significant notches are left. Once convergence is reached, say at iteration n, the PRTF spectrum embodies the resonant component alone, while a combination of the n multi-notch filters provides the reflective component. A detailed and accurate description of the separation algorithm is reported in [6].

3.2 Resonances

We now discuss the PRTF features identified by the decomposition carried out through the separation algorithm. From the 3-D plots in Figure 2 we can study how the resonances' contribution for Subjects 010 and 165 varies throughout all available elevations. The center frequency of each resonance was extracted with the help of an identification system based on a sixth-order ARMA model [15] and spatially tracked along elevation, resulting in the dotted tracks superposed on the plots.

We can easily identify two major hot-colored areas in these plots. The first one, centered around 4 kHz, appears to be very similar amongst subjects since it spans all elevations. One may immediately notice that this area includes Shaw's omnidirectional mode 1. The resonance's bandwidth appears to increase with elevation; however, knowledge of pinna modes implies that a second resonance is likely to interfere within this frequency range, specifically Shaw's mode 2 (centered around 7 kHz with a magnitude of 10 dB). On the other hand, the second hot-colored area differs both in shape and shade amongst subjects. Still it is most prominent at low elevations between 12 and 18 kHz, a frequency range which is in general agreement with Shaw's horizontal modes 4, 5, and 6.

Note that the higher resonance may be perceptually irrelevant since it lies near the upper limit of the audible range. In addition, since the resonances at 12 and 7 kHz are excited in mutually exclusive elevation ranges, we may look forward to a double-resonance filter design.

3.3 Notches

Similarly to the resonance plots, those in Figure 3 represent the frequency notches' contribution for Subjects 027 and 134. As expected, reflection patterns strongly depend on elevation and pinna shape. While PRTFs generally exhibit poor notch structures when the source is above the head, as soon as the elevation angle decreases the number and depth of frequency notches grows to an extent that varies

among subjects.

However, several analogies can be noticed here too. In order to investigate such common trends, we inherit an analysis tool that is widely used in the field of sinusoidal modeling, specifically the McAulay-Quatieri partial tracking algorithm (see [16] for details), to track the most prominent notches' patterns along all elevations. Originally, this algorithm was used to group sinusoidal partials (extracted through a peak detection algorithm) along consecutive temporal windows according to their spectral location. We implemented the original version [16] of the algorithm; obviously, since in our case elevation dependency replaces temporal evolution and spectral notches take the role of partials, we call it "notch tracking" algorithm. The notch detection step simply locates all of the local minima in the reflective component's spectrum, while the matching interval for the notch tracking procedure is set to $\Delta = 3$ kHz.

Since it is preferable to restrict our attention to the frequency range where reflections due to the pinna alone are most likely seen, and ignore notches which are overall feeble, two post-processing steps are performed on the obtained tracks:

- delete the tracks which are born and die outside the range $4 - 14$ kHz;
- delete the tracks that do not present a notch deeper than 5 dB.

The outputs of the notch tracking algorithm are the dotted tracks superposed on the plots in Figure 3. Results are definitely akin to those found in [12] with the use of an elaborated DSP-based algorithm. Three major tracks are seen for both subjects, whereas the shorter track in Subject 027's plot very probably represents the continuation of the missing track at those elevations. Reasonably, the gap between tracks is caused by the algorithm's impossibility of locating proper minima in that region (due e.g. to superposition of two different notches or the presence in the magnitude plot of valleys which are not notch-like). However, the three longer tracks suggest that similar reflection patterns occur in different PRTFs.

3.4 Reflections and anthropometry

We now move towards the definition of a realistic mapping between notch frequencies and reflection points over the pinna, by relating each major notch at frequency f_0 to a different reflection (assuming it to be the first and most prominent notch of a periodic series). Reflection models typically assume that all reflection coefficients are positive. In such case, in order for destructive interference to occur (viz. for notches to be produced in the spectrum), the extra distance travelled by the reflected wave with respect to the direct wave must be equal to half a wavelength:

$$t_d = \frac{1}{2f_0}. \tag{1}$$

This assumption was used in [12] to trace reflection points over pinna images based on the extracted notch frequencies.

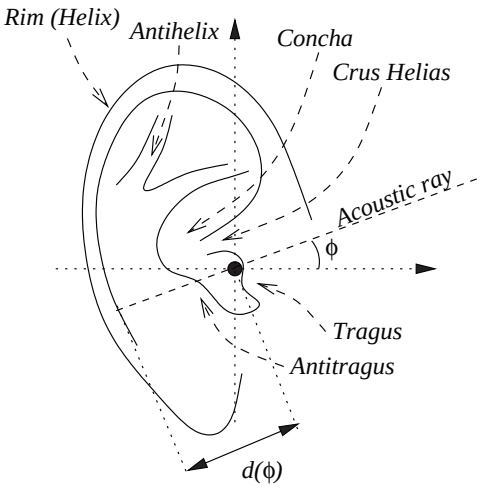

Figure 4. *Anatomy of the pinna.*

However, in [17] it was pointed out that over 80% out of a test bed of 20 CIPIC subjects exhibit a clear negative reflection in the HRIR. With the help of a simple physical model of the pinna the authors argued that, since the impedance of the pinna is greater than that of air, there may be a boundary created by an impedance discontinuity which could produce its own reflection and ultimately reverse the phase of the wave. In this latter case, a delay of half a wavelength would not produce notches in the spectrum any more. Instead, destructive interference would appear for full-wavelength delays only:

$$t_d = \frac{1}{f_0}. \tag{2}$$

We choose to use this last assumption, and relate notches to pinna geometry through a simple ray-tracing procedure similar to the one described in [12].

The distance of each reflection point with respect to the entrance of the ear canal is calculated through the following equation,

$$d(\phi) = \frac{ct_d(\phi)}{2} = \frac{c}{2f_0(\phi)}, \tag{3}$$

where $f_0(\phi)$ represents the frequency of the current notch at elevation ϕ and c is the speed of sound (approximately 343 m/s). The assumption of negative reflection coefficient causes distances to be roughly doubled with respect to those computed in [12]. Then, considering the 2-D polar coordinate system illustrated in Figure 4 with the right ear canal entrance as origin, each notch is mapped to the point $(d(\phi), \pi + \phi)$.

Results for Subject 134 are reported in Figure 5. The so-obtained mapping reveals a high degree of correspondence between calculated reflection points and pinna geometry:

- the track nearest to the ear canal very closely follows the concha wall, with a slight displacement at low elevations probably caused by the little extra distance needed by the wave to pass over the crus helias;
- the intermediate track can be associated to a reflection on the rim's edge and on the antihelix;

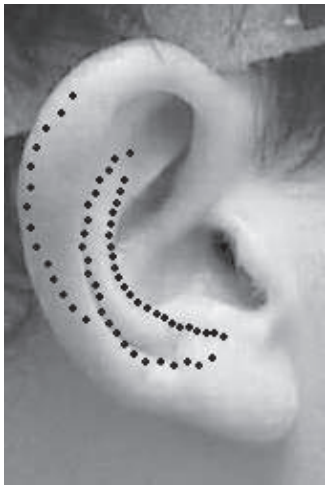

Figure 5. *Reflection points on Subject* 134*'s right pinna.*

- the furthest track follows the shape of the rim and stops in the vicinity of the point where the rim terminates, hence it is likely to be associated to a reflection in the inner wall of it.

This analysis, that yields convincing results for other subjects too, opens the door for a very attractive approach to the parametrization of the structural PRTF model based on individual anthropometry. Given a 2-D image (or possibly a 3-D reconstruction) of the user's pinna, it is possible to trace the contours of the concha wall, antihelix and rim, compute their distances with respect to the ear canal entrance, and derive the notch frequencies by reversing Eq. (3). Obviously, in order to fully justify these findings, robust theoretical motivations and a rigorous analysis using a vast test bed of subjects are required. Furthermore, since notch depth varies strongly with subjects and elevations, the reflection coefficient must also be estimated for each point.

4. A STRUCTURAL MODEL OF THE PINNA

The information gathered from the outputs of the decomposition and notch tracking algorithms allows to model the PRTF with two resonances and three spectral notches. As Figure 6 depicts, our final aim is to design two distinct filter blocks, one accounting for resonances and one for reflections. Clearly, in order to reach complete control of the filter parameters, full parametrization of the model on anthropometrical measurements is needed. Hence for the moment we shall present the PRTF re-synthesis procedure driven by the outputs of the two above algorithms.

4.1 Filter design

In Section 3.2 we have shown that a PRTF at one specific elevation includes two main resonances in the frequency range of interest for the pinna. It is then possible to approximate the effective resonances by deducing center frequency f_C and magnitude G of each resonance from the dotted tracks and directly using the so found parameters to design two second-order peak filters with fixed bandwidth $f_B = 5$ kHz of the form [18]

$$H_{res}(z) = \frac{V_0(1-h)(1-z^{-2})}{1+2dhz^{-1}+(2h-1)z^{-2}}, \tag{4}$$

where

$$h = \frac{1}{1+\tan(\pi\frac{f_B}{f_s})}, \tag{5}$$

$$d = -\cos(2\pi\frac{f_C}{f_s}), \tag{6}$$

$$V_0 = 10^{\frac{G}{20}}, \tag{7}$$

and f_s is the sampling frequency. A posteriori analysis of the synthesized resonances has revealed that PRTFs for high elevations only need the first resonance to be synthesized, being the second very close to it. We thus choose to bypass the second resonant filter when $\phi \geq 20°$.

Similarly, for what concerns the reflection block, we feed the center frequency f_C, notch depth G, and bandwidth f_B parameters coming from the notch tracking algorithm to three second-order notch filters of the form [19]

$$H_{refl}(z) = \frac{1+(1+k)\frac{H_0}{2}+d(1-k)z^{-1}+(-k-(1+k)\frac{H_0}{2})z^{-2}}{1+d(1-k)z^{-1}-kz^{-2}}, \tag{8}$$

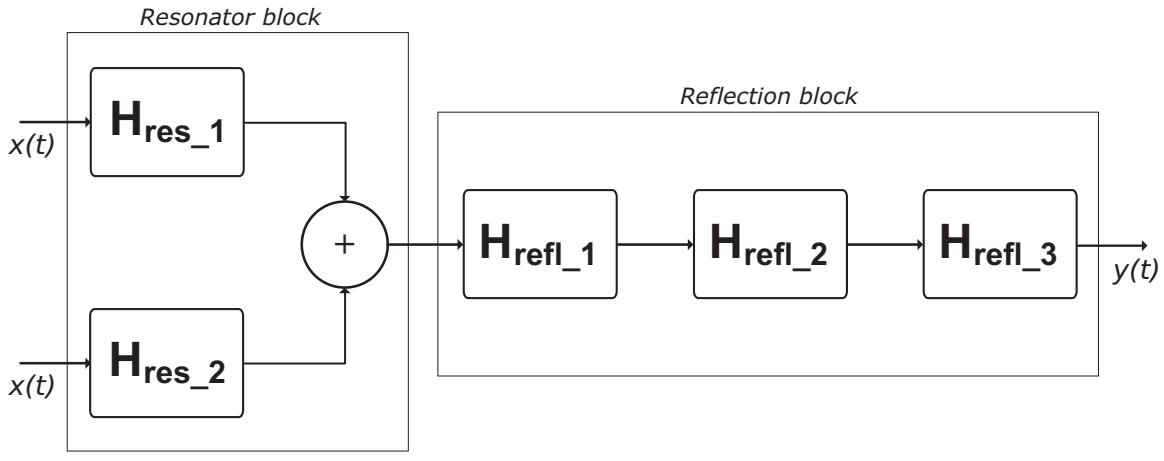

Figure 6. *General model for the reconstruction of PRTFs.*

where d is defined as in Eq. (6) and

$$V_0 = 10^{-\frac{G}{20}}, \tag{9}$$

$$H_0 = V_0 - 1, \tag{10}$$

$$k = \frac{\tan(\pi \frac{f_B}{f_s}) - V_0}{\tan(\pi \frac{f_B}{f_s}) + V_0}, \tag{11}$$

each accounting for a different spectral notch. The three notch filters must be placed in series and cascaded to the parallel of the two peak filters, resulting in an eighth-order global filter.

4.2 Results

Figure 7 reports the comparison between original and re-synthesized PRTF magnitudes for three distinct subjects, each at a different elevation. Adherence rate to the original PRTFs is overall satisfactory in the frequency range up to 14 kHz. Still, several types of imperfections need to be adjusted: as a first example, deep frequency notches that appear at low elevations complicate the notch filter design procedure. In point of fact, if the notch to be approximated is particularly deep and sharp, the second-order filter will produce a shallower and broader notch whose bandwidth may interfere with adjacent notches, resulting in underestimating the PRTF magnitude response in the frequency interval between them. Figures 7(a) and 7(b) show this behaviour around 7.5 and 10 kHz, respectively. Using a filter design procedure which forces to respect the notch bandwidth specification during re-synthesis would grant a better rendering of resonances, at the expense of worsening notch depth accuracy.

The absence of modeled notches over the upper frequency threshold is another cause of imprecision. For instance, Figure 7(a) presents an evident mismatch between original and modeled PRTF just after the 12.5-kHz peak, due to the cut of the frequency notch at 14.5 kHz. This problem may be corrected by increasing the 14-kHz threshold in order to take into account a higher number of notches. However, being the psychoacoustic relevance of this frequency range relatively low, the effective weight of the mismatch is reduced.

Last but not least, resonance modeling may bring approximation errors too. In particular, the possible presence of non-modeled interfering resonances and the fixed-bandwidth specification both represent a limitation to the re-synthesis procedure. Furthermore, center frequencies extracted by the ARMA identification method mentioned in Section 3.2 do not always coincide with peaks in the PRTF. Thus a stronger criterion for extracting the main parameters of each resonance is needed. Nevertheless, the approximation error seems to be negligible in all those cases where resonances are distinctly identifiable in the PRTF.

In conclusion, the above presented re-synthesis model appears to be overall effective, especially for PRTFs which clearly show one or two main resonant modes and moderately deep notches. Figure 7(c) supports this assertion.

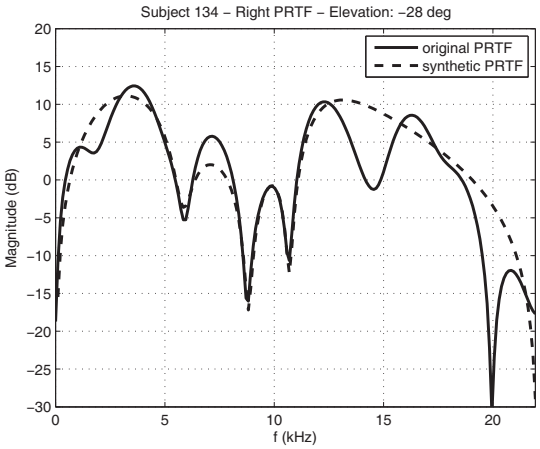

(a) Subject 134, elevation -28°.

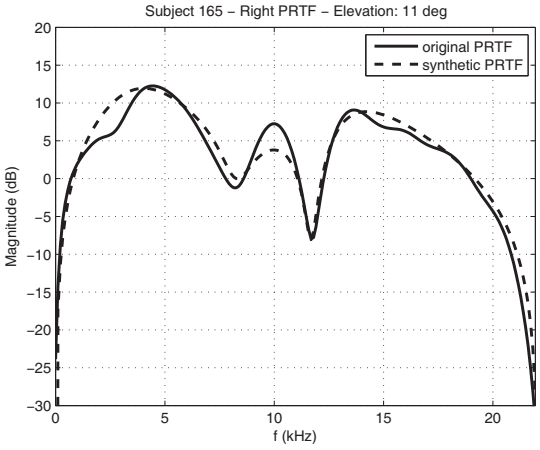

(b) Subject 165, elevation 11°.

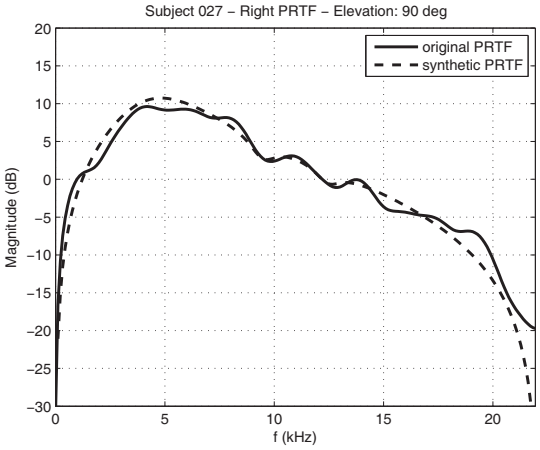

(c) Subject 027, elevation 90°.

Figure 7. *Original vs Synthetic PRTF plots.*

5. CONCLUSIONS AND FUTURE WORK

In this paper we presented an approach for structural PRTF modeling, which exploits an algorithm that separates the resonant and reflective parts of the PRTF spectrum. We used such decomposition to re-synthesize the original PRTF through a low-order filter model, whose results show an overall suitable approximation. In a parallel manner, our attempt towards the explanation of the scattering process resulting in the most important spectral notches in the PRTF provided visually convincing results. Besides improving the synthesis step, ongoing and future work includes understanding of the reflection coefficient and relating the resonant component of the PRTF to anthropometry.

6. REFERENCES

[1] J. W. Strutt, "On our perception of sound direction," *Philosophical Magazine*, vol. 13, pp. 214–232, 1907.

[2] E. C. Durant and G. H. Wakefield, "Efficient model fitting using a genetic algorithm: pole-zero approximations of HRTFs," *IEEE Transactions on Speech and Audio Processing*, vol. 10, no. 1, pp. 18–27, 2002.

[3] D. J. Kistler and F. L. Wightman, "A model of head-related transfer functions based on principal components analysis and minimum-phase reconstruction," *J. Acoust. Soc. Am.*, vol. 91, no. 3, pp. 1637–1647, 1992.

[4] C. P. Brown and R. O. Duda, "A structural model for binaural sound synthesis," *IEEE Transactions on Speech and Audio Processing*, vol. 6, no. 5, pp. 476–488, 1998.

[5] V. R. Algazi, R. O. Duda, and D. M. Thompson, "The use of head-and-torso models for improved spatial sound synthesis," in *Proc. 113th Convention of the Audio Engineering Society*, (Los Angeles, CA, USA), 2002.

[6] M. Geronazzo, S. Spagnol, and F. Avanzini, "Estimation and modeling of pinna-related transfer functions," in *Proc. of the 13th Int. Conference on Digital Audio Effects (DAFx-10)*, (Graz, Austria), September 6-10 2010. Accepted for publication.

[7] D. W. Batteau, "The role of the pinna in human localization," *Proc. R. Soc. London. Series B, Biological Sciences*, vol. 168, pp. 158–180, August 1967.

[8] A. J. Watkins, "Psychoacoustical aspects of synthesized vertical locale cues," *J. Acoust. Soc. Am.*, vol. 63, pp. 1152–1165, April 1978.

[9] K. J. Faller II, A. Barreto, N. Gupta, and N. Rishe, "Time and frequency decomposition of head-related impulse responses for the development of customizable spatial audio models," *WSEAS Transactions on Signal Processing*, vol. 2, no. 11, pp. 1465–1472, 2006.

[10] E. A. G. Shaw, *Binaural and Spatial Hearing in Real and Virtual Environments*, ch. Acoustical features of human ear, pp. 25–47. Mahwah, NJ, USA: R. H. Gilkey and T. R. Anderson, Lawrence Erlbaum Associates, 1997.

[11] N. Gupta, A. Barreto, and M. Choudhury, "Modeling head-related transfer functions based on pinna anthropometry," in *Proc. of the Second International Latin American and Caribbean Conference for Engineering and Technology (LACCEI)*, (Miami, FL, USA), 2004.

[12] V. C. Raykar, R. Duraiswami, and B. Yegnanarayana, "Extracting the frequencies of the pinna spectral notches in measured head related impulse responses," *J. Acoust. Soc. Am.*, vol. 118, pp. 364–374, July 2005.

[13] P. Satarzadeh, R. V. Algazi, and R. O. Duda, "Physical and filter pinna models based on anthropometry," in *Proc. 122nd Convention of the Audio Engineering Society*, (Vienna, Austria), May 5-8 2007.

[14] R. V. Algazi, R. O. Duda, D. M. Thompson, and C. Avendano, "The CIPIC HRTF database," in *IEEE Workshop on Applications of Signal Processing to Audio and Acoustics*, (New Paltz, New York, USA), pp. 1–4, 2001.

[15] P. A. A. Esquef, M. Karjalainen, and V. Välimäki, "Frequency-zooming ARMA modeling for analysis of noisy string instrument tones," *EURASIP Journal on Applied Signal Processing: Special Issue on Digital Audio for Multimedia Communications*, no. 10, pp. 953–967, 2003.

[16] R. J. McAulay and T. F. Quatieri, "Speech analysis/synthesis based on a sinusoidal representation," *IEEE Transactions on Acoustics, Speech, and Signal Processing*, vol. 34, no. 4, pp. 744–754, 1986.

[17] P. Satarzadeh, "A study of physical and circuit models of the human pinnae," Master's thesis, University of California Davis, 2006.

[18] S. J. Orfanidis, ed., *Introduction To Signal Processing*. Prentice Hall, 1996.

[19] U. Zölzer, ed., *Digital Audio Effects*. New York, NY, USA: J. Wiley & Sons, 2002.